# Hydrogenolysis of Glycerol to Propylene Glycol: Energy, Tech-Economic, and Environmental Studies

Puhua Sun[1], Wenxiang Zhang[1], Xiao Yu[1], Jie Zhang[1], Ningkun Xu[1], Zhichao Zhang[1], Mengyuan Liu[1], Dongpei Zhang[1], Guangyu Zhang[2], Ziyuan Liu[1], Chaohe Yang[1], Wenjuan Yan[1]* and Xin Jin[1]*

[1]State Key Laboratory of Heavy Oil Processing, College of Chemical Engineering, China University of Petroleum, Qingdao, China, [2]Sinopec Research Institute of Safety Engineering, Qingdao, China

Hydrogenolysis of glycerol to propylene glycol represents one of the most promising technologies for biomass conversion to chemicals. However, conventional hydrogenolysis processes are often carried out under harsh $H_2$ pressures and temperatures, leading to intensive energy demands, fast catalyst deactivation, and potential safety risks during $H_2$ handling. Catalytic transfer hydrogenolysis (CTH) displays high energy and atom efficiency. We have studied a series novel solid catalysts for CTH of glycerol. In this work, detailed studies have been conducted on energy optimization, tech-economic analysis, and environmental impact for both processes. The key finding is that relatively less energy demands and capital investment are required for CTH process. $CO_2$ emission per production of propylene glycol is much lower in the case of transfer hydrogenolysis. The outcome of this study could provide useful information for process design and implementation of novel hydrogenolysis technologies for other energy and environmental applications.

Keywords: hydrogenolysis, biomass, comparative study, assessment, glycerol, propylene glycol

## INTRODUCTION

Aqueous phase hydrogenolysis of bio-oxygenates provides a most promising technology for the production of various megaton chemicals from renewable feedstocks. (Wang et al., 2015a; Jin et al., 2019a; Park et al., 2021). In this context, hydrogenolysis of polyols to glycols and alcohols could offer alternative synthetic routes and alleviate the use of hydrocarbons for energy-intensive conversion processes. In particular, hydrogenolysis of glycerol, a bio-diesel by-product, can produce propylene glycol (PG), 1,3-propanediol, ethylene glycol (EG), as well as propanols for many downstream applications such as anti-freezes, polyesters, pharmaceuticals, and solvents. This is one of the most popular subjects which is under extensive studies in both academia and industry. (Haldar and Mahajani, 2004; Guo et al., 2009). However, hydrogenolysis of glycerol is often conducted under elevated temperatures and $H_2$ pressures (>230°C, >4 MPa). Actually, this process is still heavily dependent on the use of fossil-derived $H_2$, with cost-ineffective investment on $H_2$ compression, recycling, and manufacture of process equipment. (Humbird et al., 2017; Freitas et al., 2018). It is true that renewable $H_2$ ("green $H_2$") can now be produced from other feedstocks, e.g., electrolysis of water. But one should note that most hydrogenation plants have to be established adjacent to $H_2$

**Graphical Abstract |** Table of Content Graph: Process analysis for conventional hydrogenolysis and transfer hydrogenolysis of glycerol reveals the energy, economic and environmental impact on biomass conversion.
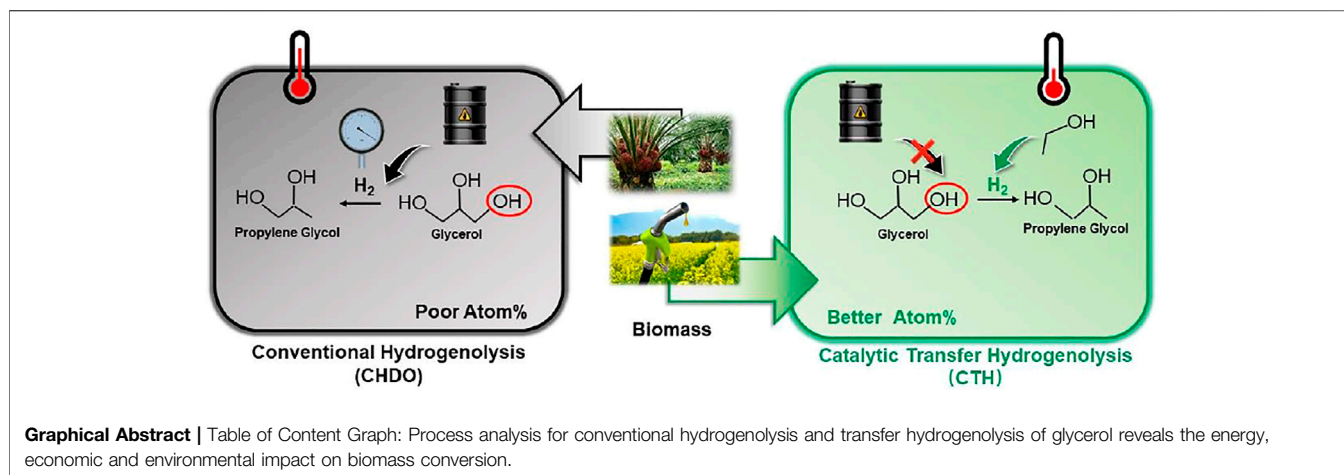
source or pipelines, which could unfavorably increase operational and constructional cost for biorefineries. In addition, potential safety risk is another important factor hindering industrial implementation of this technology. Advanced aqueous phase hydrogenolysis technologies with low-carbon emission are highly demanded for future development of bio-refineries.

Catalytic transfer hydrogenolysis (CTH), which takes use of renewable H-donors in liquid medium, is considered as one of the most economically and environmentally beneficial technique to substitute conventional hydrogenolysis processes (CHDO, **Figure 1**). (Jin et al., 2019b; Zhang et al., 2020a; Yin et al., 2020; Nie et al., 2021). Much milder reaction temperatures, higher intrinsic hydrogenolysis rates in aqueous medium, and lower operating pressures in the absence of externally added $H_2$ make CTH processes more energy and atom efficient compared with CHDO processes. Extensive research efforts have been devoted to develop active and selective solid catalyst materials with bifunctional natures for both $H_2$ generation and hydrogenolysis reactions. Pt-based (Tike and Mahajani, 2006; Falcone et al., 2015; Feng et al., 2015; Von Held Soares et al., 2017; Zhang et al., 2020b; Hu et al., 2020; Xia et al., 2020; Nie et al.,

2021; Song et al., 2021), Cu-based (Nie et al., 2021; Feng et al., 2015; Wang et al., 2015b; Priya et al., 2016; Feng et al., 2011; Kant et al., 2017; Vasiliadou and Lemonidou, 2013; A et al., 2017), and Pd-based (Tike and Mahajani, 2006; Feng et al., 2015; Mauriello et al., 2015; Sun et al., 2017; Shafaghat et al., 2019; Xia et al., 2020; Song et al., 2021) catalysts have been proposed and investigated with respect to structure-performance relations. Those studies have confirmed that CTH of glycerol can be achieved under milder temperatures (<200°C) and pressures (inert <2 MPa), with remarkable atom efficiency for the synthesis of PG as the main product (Wang et al., 2013; Feng et al., 2015). Experimental studies have demonstrated the feasibility of CTH technique for catalytic upgrading of glycerol as well as other bio-oxygenates.

However, to our best knowledge, limited studies on energy, economic, and environmental assessment (E3A) have been carried out to evaluate the overall impact of CTH processes particularly for the production of PG from glycerol (D'Angelo et al., 2018; Gonzalez-Garay et al., 2017). This study is very important, as it will provide the overall energy efficiency, greenhouse gas emission, and economic advantages of CTH processes. More critically, the hot spot detected in E3A studies
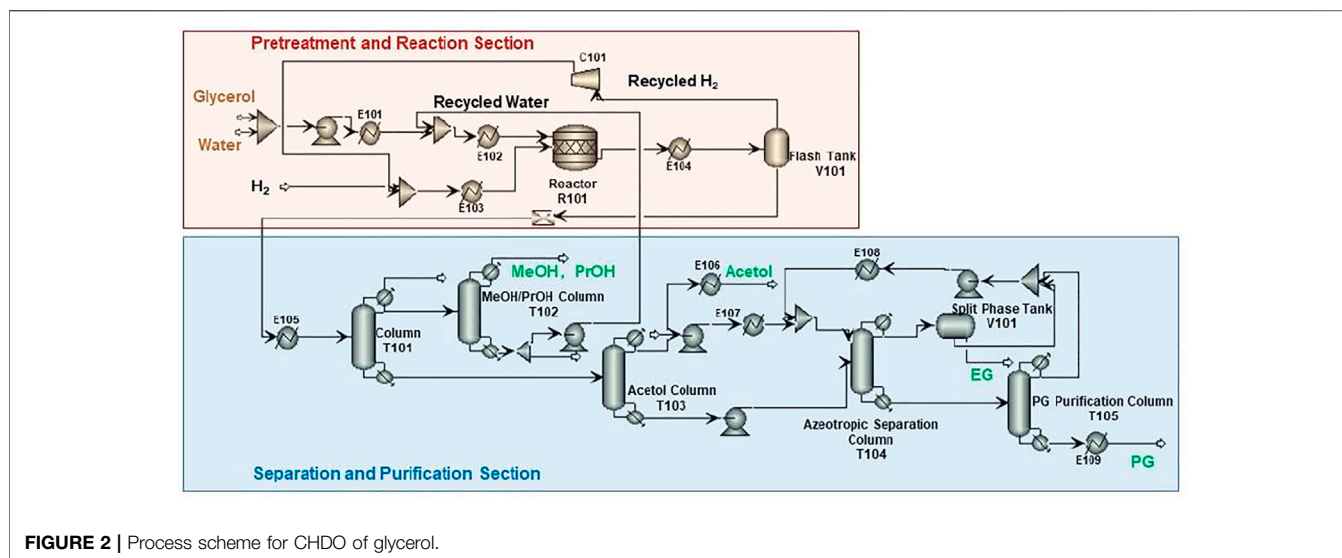


**FIGURE 1 |** Conventional HDO (CHDO) and catalytic transfer hydrogenolysis (CTH).
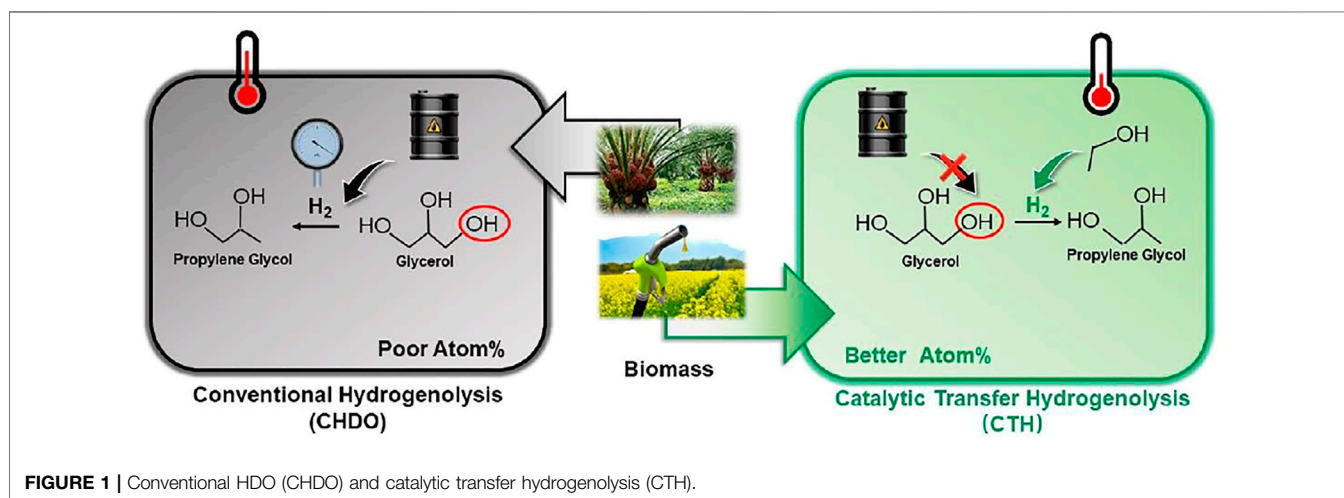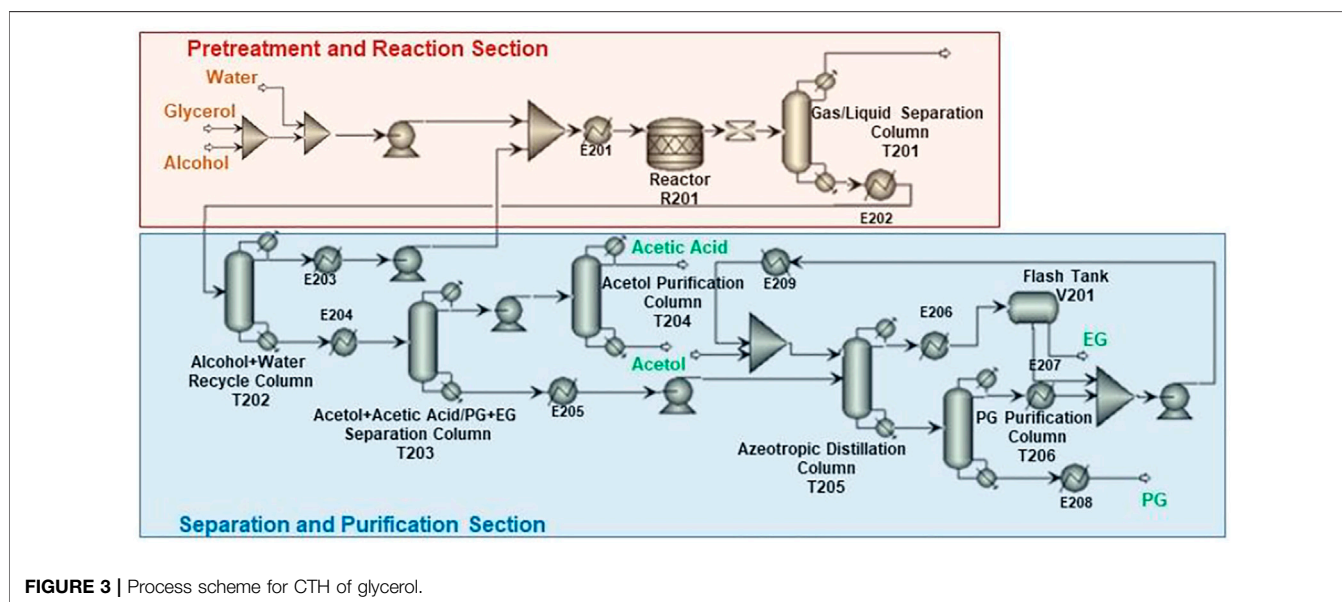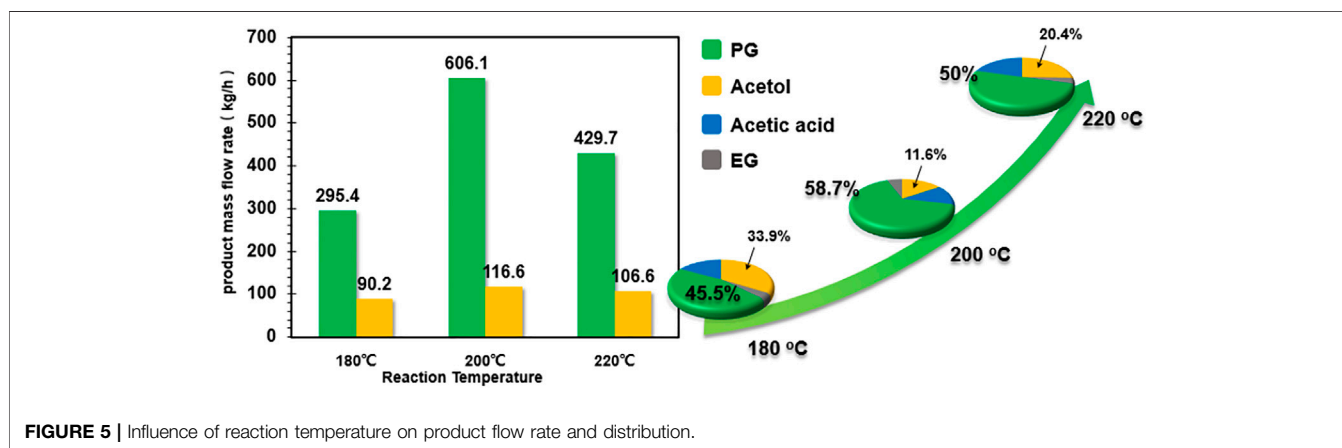
**FIGURE 2 |** Process scheme for CHDO of glycerol.



**FIGURE 3 |** Process scheme for CTH of glycerol.

**TABLE 1 |** Reactions of CTH scheme.

| Main products | Selectivity (%) |
| --- | --- |
| PG | 58.7 |
| Acetic acid | 13.9 |
| Acetol | 11.6 |
| EG | 5.1 |

will also offer insights into process optimization in terms of energy and capital investment (D'Angelo et al., 2018; Arpia et al., 2021; Beneroso et al., 2017; Wicker et al., 2021; Xiang et al., 2014; Zaimes et al., 2015; Zhao et al., 2021) to further reduce the carbon-footprint and operating cost for facile production of PG.

However, to our best knowledge, no relevant reports have been published on comparative studies of energy, economy, and environmental assessment for both CHDO and CTH of glycerol. Therefore, in this work, we reported a detailed and comparative study on CHDO and CTH of glycerol to PG. Specifically, 1) energy consumptions for glycerol pretreatment, hydrogenolysis reactors, and separation/purification sections have been compared for both CHDO and CTH. Heat exchange network has also been optimized. 2) Economic analysis on how reduction of $H_2$ compression contributes to overall economic improvement has been conducted. 3) Environmental analysis has also been carried out to estimate the $CO_2$ emission and water discharge for both processes, respectively. Finally, both advantages and disadvantages for

**FIGURE 4 |** Product distribution and mass flow rate for **(A)** CHDO and **(B)** CTH of glycerol.



**FIGURE 5 |** Influence of reaction temperature on product flow rate and distribution.
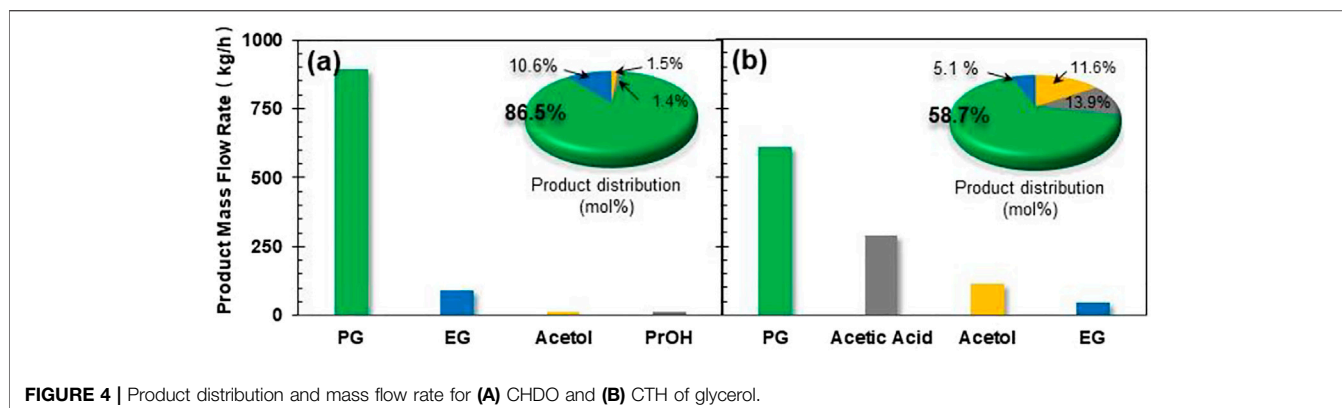
CTH of glycerol have been quantitatively discussed for future design of next-generation bio-refineries.
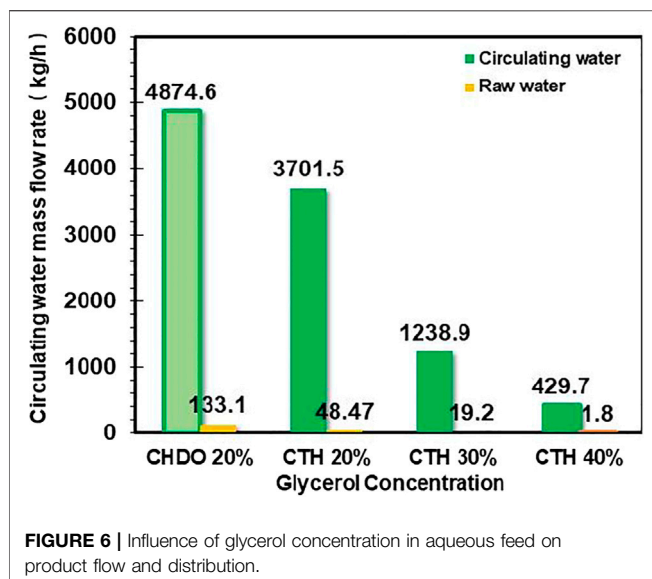
## METHODOLOGY

### Thermodynamic Model

In this work, the following chemicals have been incorporated for process simulation, water, glycerol, ethyl alcohol, propylene glycol (PG), propanol (PrOH), ethylene glycol (EG), acetol, cycloheptane, methanol (MeOH), ethanol (EtOH), acetic acid, $CH_4$, $H_2$, and $CO_2$. Redlich-Kwong and NRTL models were adopted for simulation. Redlich-Kwong model was used to determine gas composition, while NRTL method was used to describe liquid phase (Rocha et al., 2014; Li et al., 2016; Liu et al., 2018). Since reaction and separation units involve gas-liquid and liquid-liquid multiphase system in this work, NRTL (non-random two liquid) model is supposed to be well predictive in determining the actual composition of various components (Poozesh et al., 2015; Li et al., 2016; Mirzaei et al., 2016; Xie et al., 2016; Hernández et al., 2018; Ma et al., 2018; Ma et al., 2019; Qin et al., 2019; Chen et al., 2020).

Redlich-Kwong and NRTL models are only suitable for polar and gas-liquid phase systems. Tech-Economic analysis has been focused on utilities and capital investment. There are many empirical parameters which may generate large errors. However, those errors are acceptable for engineering design.

## Technical Approach and Process Simulation

Both CHDO and CTH plant studied in this work consist of three main units: pretreatment unit, hydrogenolysis unit where glycerol is converted into PG and other co-products, and separation and purification unit. In this work, reaction results over Ni/Cu/TiO$_2$ catalyst were used for simulation of CHDO process (Cai et al., 2018; Jin et al., 2019a; Jin et al., 2019b; Xia et al., 2020; Yin et al., 2020). Ni/Cu/TiO$_2$ catalyst was selected for CHDO process because it displays leading performances in conversion and PG selectivity in literature. It has been a widely accepted catalyst material for numerous hydrogenation applications. Results obtained from PtFe-based catalyst, which were reported in recent work, were selected as the reaction model to simulate CTH process (Zhang et al., 2020a). Compared with other investigated catalysts for transfer hydrogenolysis reaction, PtFe-based catalyst displays much higher activity, although selectivity towards PG (58.7%) can be still improved in future studies.

Process scheme for CHDO of glycerol is presented in **Figure 2**. It is seen that this scheme consists of three major units,

**FIGURE 6 |** Influence of glycerol concentration in aqueous feed on product flow and distribution.

pretreatment unit and reaction unit, followed by separation and purification unit. Glycerol, water, and $H_2$ are mixed with a ratio of 1:20:10 (molar) and fed to the reactor (R101 in **Figure 2**), where hydrogenolysis reaction is conducted under 230°C and 3.5 MPa $H_2$ pressure. The main products include PG, PrOH, MeOH, and acetol, with chemoselectivity being 86.5, 1.5, 10.6, and 1.4%, respectively. The separation sequence for CHDO includes primary separation (T101), MeOH/PrOH separation (T102), acetol purification (T103), azerotropic separation (T104), and PG purification units (T105). Cycloheptane is used as azerotropic agent and recovered from T104 and T105 (Dohnal et al., 2014).

**Figure 3** presents the process scheme for CTH of glycerol, which also consists of pretreatment unit, reaction unit, and purification unit. Glycerol is fed with EtOH (H-donor) as the feedstock into the reactor. Glycerol/EtOH/$H_2O$ (69.7/24.8/0.5 M ratio), together with recycling water, is pumped into reactor (R201 in **Figure 3**). The reaction effluent is first flashed in a Gas/Liquid Separation Column (T201) in this scheme to separate gas components such as trace amounts of $H_2$ and $CO_2$ from reaction mixture. EtOH and water are recycled into the reactor in Alcohol + Water Recycle Column (T202), in which the raw material could be saved. After being separated in Acetol + acetic acid/PG + EG Separation Column (T203), Acetol is purified in Acetol Purification Column (T204), while PG is purified in azeotropic distillation system including Azeotropic Distillation Column (T205) and PG Purification Column (T206).

## Reaction Scheme for CTH Process

Reaction parameters such as temperatures, pressures, and catalyst loading have been studied experimentally in our laboratory, as already reported previously (Jin et al., 2019a; Jin et al., 2019b; Zhang et al., 2020a; Zhang et al., 2020b; Yin et al., 2020). Conversion and selectivity data obtained from those reports were used as input for determination of configuration of reactor unit in simulation (Von Held Soares et al., 2017; Zhang et al., 2020a; Yin et al., 2020). As shown in **Table 1**,

the reactions considered for this work include 1) dehydrogenation of EtOH, 2) dehydration of glycerol, and (3–4) hydrogenolysis of glycerol. More details of reactor design are presented in supporting information Reactor Design.

## Models

Rstoic model was applied for the hydrogenolysis reactor. In separation and purification section, the main unit operations are fractionation and azeotropic distillation; thus, the RadFrac model was used. This model could be used for accurate calculation of each column (Humbird et al., 2017; Pla-Franco et al., 2019). Properties for major components were summarized in **Supplementary Table S1, S2** for setting up separation sequences and further optimization. Aspen Energy Analyzer was used to carry out optimization of heat exchange network (refer to **Supplementary Figure S5** for more details).

## Economic Analysis

In this part, calculation of investment, capital cost, and revenue was conducted for CHDO and CTH process. The capital cost for manufacturing and facilities is defined as the total direct capital cost (TDC) (Xiang et al., 2014; Zhou et al., 2019; Saavedra del Oso et al., 2020) which is estimated by the production capacity index approach, and it is defined as:

$$TDC = \sum_{i=1}^{m} C_{E,i} = \sum_{i=1}^{m} C_{basic}\left(\frac{Q}{Q_{basic}}\right)^{\alpha} f \qquad (1)$$

where m is the total unit in process design, $C_{E,i}$ is the capital cost of each process corresponding to actual capacity Q, $C_{basic}$ indicates the capital cost with the base case capacity, α is the cost scale factor, and f is a comprehensive adjustment factor (Zhou et al., 2019; Cormos, 2021; Marchese et al., 2021). $Q/Q_{basic}$ is 1/1 for both CHDO and CTH processes, the ratio of which was determined based on previous literature (Zhou et al., 2019; Cormos, 2021; Marchese et al., 2021). Details about equipment costs are presented in **Supplementary Table S8, S9** of supporting information. Therefore, the indirect plant expense (IPE) is estimated as 30% of TDC, which consists of the capital costs for engineering and supervision, start-up capital, spares costs, construction expenses, contractor fees, and other contingency cost. TDC and IPE are combined to estimate the total plant capital cost (TPC) of CHDO and CTH scheme, which is defined as:

$$TPC = TDC + IPE \qquad (2)$$

The capital cost summary of CHDO and CTH scheme is shown in **Table 5**. More details are talked in results and discussion.

## Environmental Analysis

In this part, environment analysis is mainly focused on evaluating and comparing the environmental impacts of producing PG from CHDO and CTH processes. The environment analysis includes direct and indirect emission of $CO_2$, the effluent discharge, the organic compounds, and equivalent greenhouse gas emissions in

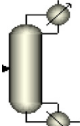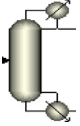**TABLE 2 |** Energy consumption of main equipment in CTH process at different concentration of glycerol.
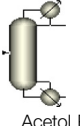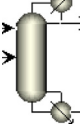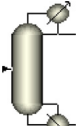
| Three different concentration of glycerol | 20wt% | 30wt% | 40wt% |
|---|---|---|---|
| **Equipment** | | | |
| R201 <br> Catalytic transfer Hydrogenolysis Reactor | 430.4 | 352.3 | 300.8 |
| T201 <br> Gas/Liquid Separation Column | 14,631.3 | 12,310.3 | 11,241.5 |
| T202 <br> Alcohol + Water Recycle Column | 21,308.9 | 10,510.7 | 9,718.4 |
| T203 <br> Acetol + acetic acid/PG + EG Separation Column | 614.7 | 609.4 | 605.4 |
| T204 <br> Acetol Purification Column | 261.2 | 255.4 | 252.5 |
| T205 <br> Azeotropic Distillation Column | 5,501.5 | 5,560.5 | 5,669.5 |
| T206 <br> PG Purification Column | 173.9 | 168.3 | 175.9 |
| Total Heat Demand (kW) | 42,821.9 | 29,766.9 | 27,964.1 |

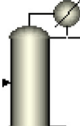**TABLE 3 |** Energy consumption of main equipment in CTH process at different concentration of glycerol.

| Three different reaction of temperature | 180°C | 200°C | 220°C |
|---|---|---|---|
| **Equipment** | | | |
| R201 — Catalytic transfer Hydrogenolysis Reactor | 95.9 | 352.3 | 870.5 |
| T201 — Gas/Liquid Separation Column | 10.511.4 | 12,310.3 | 11,794.3 |
| T202 — Alcohol + Water Recycle Column | 11,010.5 | 10,510.7 | 12.028.2 |
| T203 — Acetol + acetic acid/PG + EG Separation Column | 756.1 | 609.4 | 707.4 |
| T204 — Acetol Purification Column | 364.3 | 255.4 | 359.9 |
| T205 — Azeotropic Distillation Column | 5,214.2 | 5,560.5 | 5,331.9 |
| T206 — PG Purification Column | 163.5 | 168.3 | 166.4 |
| Total Heat Demand (kW) | 28,115.8 | 29,766.9 | 31,258.5 |

**FIGURE 7 |** Power consumption of CHDO and CTH scheme.
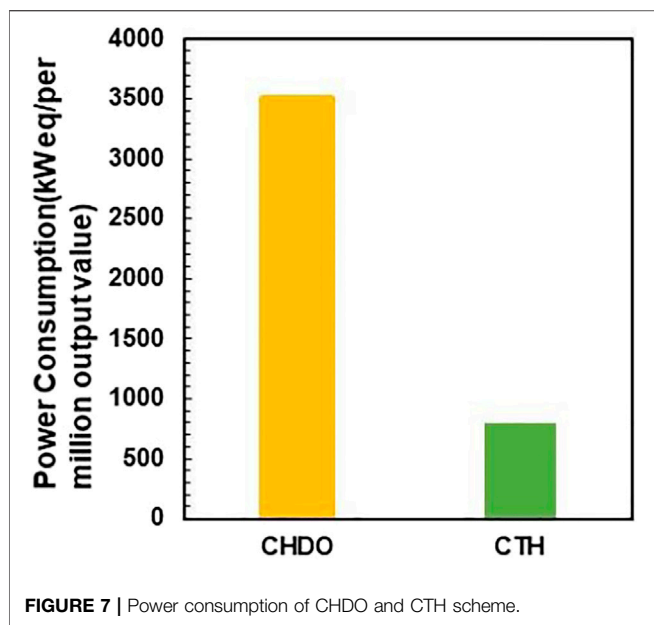
CHDO and CTH process. The quantitative analysis is reported according to million $ production (Saavedra del Oso et al., 2020).

As the main greenhouse gas (GHG), $CO_2$ emissions can be calculated by the sum of direct emissions and indirect emissions. The direct emissions are mainly from reactions such as "$C_3H_8O_3 + 3H_2O = 3CO_2 + 7H_2$" and the process emissions, while the indirect emissions are caused by process energy production such as steam for heating and electricity for driving equipment.

## RESULTS AND DISCUSSION

### General Information on CHDO Process

Prior to detailed comparative studies for both CHDO and CTH processes, it is important to set up the reference operating conditions for systematic investigation. Despite extensive studies on CHDO processes, there is lack of experimental

kinetic data for the leading $Ni/Cu/TiO_2$ catalyst in literature. As a result, the operating conditions for $Ni/Cu/TiO_2$ catalyst in CHDO of glycerol cannot be optimized in this work. Such optimization would not be reliable without kinetic data under different temperatures and pressures from experimental studies. Therefore, the operating conditions $Ni/Cu/TiO_2$ catalyst.

### Process Schemes

It is important to mention that $H_2$ is recycled and compressed in this scheme (V101). To simplify the scheme, we have reduced the purification part for $H_2$ recycling for the convenience of further cost estimation. It is also critical that, for CHDO process, we already found that recycling water is not economically viable as the cost for $H_2$ purification. Those preliminary calculations showed that $H_2O$ recirculation and $H_2$ purification are not expedient from the technological point of view, and therefore, they are excluded from the technological schemes.

Different from CHDO process, CTH of glycerol is composed of relatively simpler scheme. $H_2$ compression unit is not required, as there is no external $H_2$ added in CTH of glycerol. However, glycerol should be fed with EtOH (H-donor) as feedstock into the reactor. Glycerol/EtOH/$H_2O$ (69.7/24.8/0.5 M ratio) is pumped into reactor (R201 in **Figure 3**) for CTH reactions. This ratio is pre-determined based on our previous report for experimental studies. The reaction effluent is first flashed in a gas/liquid separation column (T201), then gas components such as trace amounts of $H_2$ and $CO_2$ from reaction mixture are separated. Light components including $CH_4$, $H_2$, $CO_2$, and trace MeOH were sent to furnace for combustion. Another difference for CTH of glycerol, compared with CHDO process, is the separation unit. In CTH of glycerol, the main products, as described in previous sections, include PG, EG, acetol, acetic acid, and MeOH, leading to distinct separation scheme for the proposed process. In particular, alcohol + water mixture (EtOH/MeOH/$H_2O$: 29/4.6/66.4 M ratio) is recycled back with fresh feedstock with Glycerol/EtOH/$H_2O$ stream. The remaining unreacted alcohols can be used as H-donor for fresh feedstocks. For CTH process, dehydration of glycerol leads to the formation of acetol, while dehydrogenation of EtOH eventually generates acetic acid as the

**TABLE 4 |** Energy summary of CHDO and CTH scheme.

| Process | | | CHDO (kW) | | CTH (kW) | |
|---|---|---|---|---|---|---|
| **Energy consumption** | | | | | | |
| 1 | Pretreatment Section | | 175.1 kW | | 149.5 kW | |
| 2 | Reaction Section | | 2,247.4 kW | | 430.4 kW | |
| **3** | Separating and Purification Section | T101[a] | | 39,398.0 kW | T201[#] | 14,631.3 kW |
| | | T102[a] | | 1,742.6 kW | T202[#] | 21,308.9 kW |
| | | T103[a] | | 332.5 kW | T203[#] | 614.7 kW |
| | | T104[a] | | 7,019.5 kW | T204[#] | 261.2 kW |
| | | T105[a] | | 1,024.5 kW | T205[#] | 5,501.5 kW |
| | | V101[a] | | 80.3 kW | T206[#] | 173.9 kW |
| | | Sum | | 49,597.4 kW | Sum | 42,491.5 kW |
| 4 | Total Consumption | | 52,019.9 kW | | 43,071.4 kW | |

[a]T101, Column *T102 MeOH/PrOH column; *T103, Acetol Column *T104 Azeotropic Separation Column; *T105, PG purification column; *T201, Gas/Liquid Separation Column; *T202, Alcohol + Water Recycle Column; *T203, Acetol + acetic acid/PG + EG separation column; *T204, Acetol Purification Column; *T205, Azeotropic Distillation Column; *T206, PG purification column.
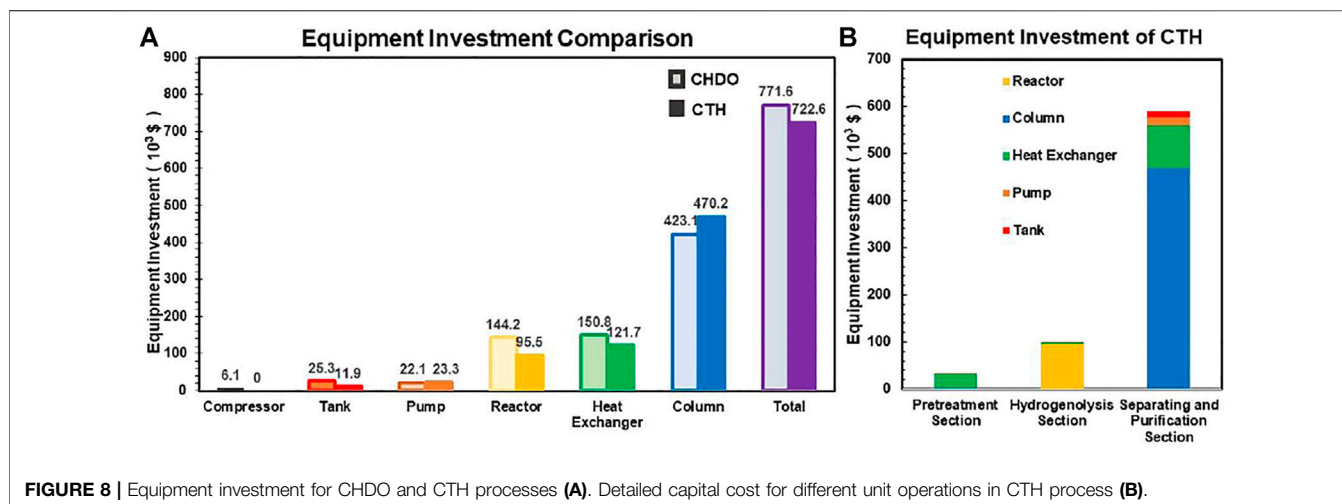
**FIGURE 8 |** Equipment investment for CHDO and CTH processes **(A)**. Detailed capital cost for different unit operations in CTH process **(B)**.

final product. Acetol and acetic acid are separated from PG and EG in T203, while acetol could be further obtained in T204 with 99.95% purity. Similar to CHDO scheme, PG and EG are separated using azeotropic distillation sequence (T205-T206, refer to supporting information for more details).

Based on description presented above, it is clear that, for CTH of glycerol, $H_2$ cycling and product separation units are completely different from the conventional one. Therefore, we were motivated to further study the advantages and possible disadvantages of CTH technology for glycerol conversion in the following sections.

## Detailed Studies on Process Parameters for Both Processes

Prior to detailed investigation on the influence of process parameters on productivity and energy/capital costs, we first compared the product flow rate and composition for CHDO and CTH processes. The mass flow rates for PG, EG, acetol, and PrOH are 893.4 kg/h, 89.3 kg/h, 14.1 kg/h, and 12.3 kg/h, respectively, while CTH of glycerol leads to 606.3 kg/h, 42. kg/h, and 116.6 kg/h for those products. The product distribution (carbon-based selectivity, 58.7%) (Zhang et al., 2020a; Yin et al., 2020) for the two processes has also been presented in inset of **Figure 4**. It is found that, for CHDO process, the main products include PG (86.5%) and EG (10.6%), with trace amounts of acetol and PrOH as co-products. Interestingly, for CTH of glycerol using EtOH as H-donor, the main products are PG (58.7%), acetic acid (13.9%), and acetol (11.6%). Clearly, the product distribution from the two processes is distinct from each other. This is because that for CTH process, $H_2$ generation from EtOH as H-donor leads to the formation of acetic acid in the reaction medium, while conversion of glycerol undergoes dehydration and hydrogenolysis steps, forming acetol and PG as intermediate and final products, respectively.

The influence of temperature on product distribution and product mass flow rate is presented in **Figure 5**. It is observed that increasing reaction temperature from 180°C to 200°C leads to

**TABLE 5 |** Capital cost of CHDO and CTH scheme.

| Items [10 (Jin et al., 2019a) $] | CHDO | CTH |
|---|---|---|
| Total Direct Cost (TDC) | 1,234.6 | 1,155.4 |
| Indirect Plant Expenses (IPE) | 370.4 | 346.6 |
| Total Plant Capital Cost (TPC) | 1,605 | 1,502 |

improved selectivity to PG from 45.5 to 58.7%, with decreasing selectivity for acetol from 33.9 to 11.6%. However, further increasing temperature to 220°C causes significant degradation reactions with $CH_4$ and $CO_2$ as by-products. As a result, the overall product mass flow rates for PG and acetol are much lower than that at 200°C.

We also studied the influence of glycerol concentration on the amount of total recycled water for CTH scheme. It is found from **Figure 6** that increasing glycerol concentration from 20wt% to 40wt% in the feedstock leads to significant changes of water consumption. In particular, the CTH process with 20wt% glycerol concentration in the feedstock demands 2014.2 kg/h and 1735.8 kg/h of recycling water and additional water input, respectively. As glycerol concentration enhanced to 30wt%, we confirmed that the water demands for CTH process have been decreased dramatically, down to 1,238.9 kg/h and 19.2 kg/h, respectively, for recycling water and additional water input.

In this part of work, simulation of glycerol concentration effect on CHDO process could not be conducted due to lack of kinetic data in literature. It would be very useful to compare the concentration effect for both schemes, providing more critical insights into the sustainability of CHDO and CTH processes. Therefore, 20wt% glycerol concentration was still used for further comparison of two schemes to ensure consistency in processing capability of the two technologies.

It is also important to mention that the water generated in both CHDO and CTH meets the environment regulation for discharge. Therefore, CTH processes with much lower water demand is more favorable for lowering the overall cost of water treatment.

**TABLE 6 |** Sale revenue for CHDO and CTH process.

| Scheme | CHDO | CTH | | | |
|---|---|---|---|---|---|
| **Product** | **PG** | **PG** | **Acetol** | **EG** | **Acetic acid** |
| Annual Output (ton/a) | 7,141.2 | 4,850.3 | 927.2 | 343.7 | 2,316.6 |
| Purity (wt%) | 99.9 | 99.9 | 99.1 | 99.9 | 99.5 |
| Sales Revenue (10 Jin et al. (2019a) $) | 14,830 | 10,080 | 43,400 | 186 | 1,070 |
| Sales Total (10 Jin et al. (2019a) $) | 14,830 | 54,736 | | | |

Based on the comparison shown above, it is clear that CTH process displays the following advantages:

1) Higher atom efficiency for value-added PG and acetol products. Considering the use of external pressurized $H_2$ with high $H_2$/glycerol ratio (10), for CHDO processes, utilization of stoichiometric liquid H-donors exhibits much better overall atom economics.
2) Lower water input. Based on **Figure 6**, the water demands for recycling and additional input are approximately 74.8% compared with CHDO process with 20wt% glycerol concentration in the feedstock.

The interesting results in **Figure 6** provide further insights into nature of reaction network for both processes. For CHDO process, water is solvent and a by-product, while water is both reactant and product for CTH scheme. This is the reason that CHDO process needs additional water to provide reaction medium.

In the following sections, we will further discuss the energy demands for CHDO and CTH processes, which provide important evaluation for the economics and profit analysis.

## Influence of Glycerol Concentration and Temperature for CTH Process

Glycerol concentration will influence the reaction kinetics as well as separation cost. This is because glycerol concentration will influence the amount of recirculating water as well as the heat duty for each of the downstream separation column. In this section, energy requirement for CHDO and CTH under identical glycerol concentration will be compared prior to detailed investigation on how glycerol concentration in the feed affect energy cost for CTH scheme. The amount of water (solvent) used in this system under different glycerol concentration varies significantly from 20wt% to 40wt%, as already seen in **Figure 6**. In particular, altering glycerol concentration from 20wt% to 40wt% not only modifies the intrinsic conversion rate of glycerol in the presence of PtFe/Y catalysts but also changes the conversion rate of H-donor (EtOH) in aqueous medium. Increasing glycerol concentration undoubtedly decreases the overall water consumption in CTH process, thus further leading to lowered energy input. As found in **Table 2**, the energy requirement for R201, T201-206 is 430.4 kW, 14,631.3, 21308.9, 614.7, 261.2 kW, 5,501.5 kW, and 173.9 kW, respectively, contributing to a total of 42,822 kW under this scenario. Significantly, when glycerol concentration enhanced
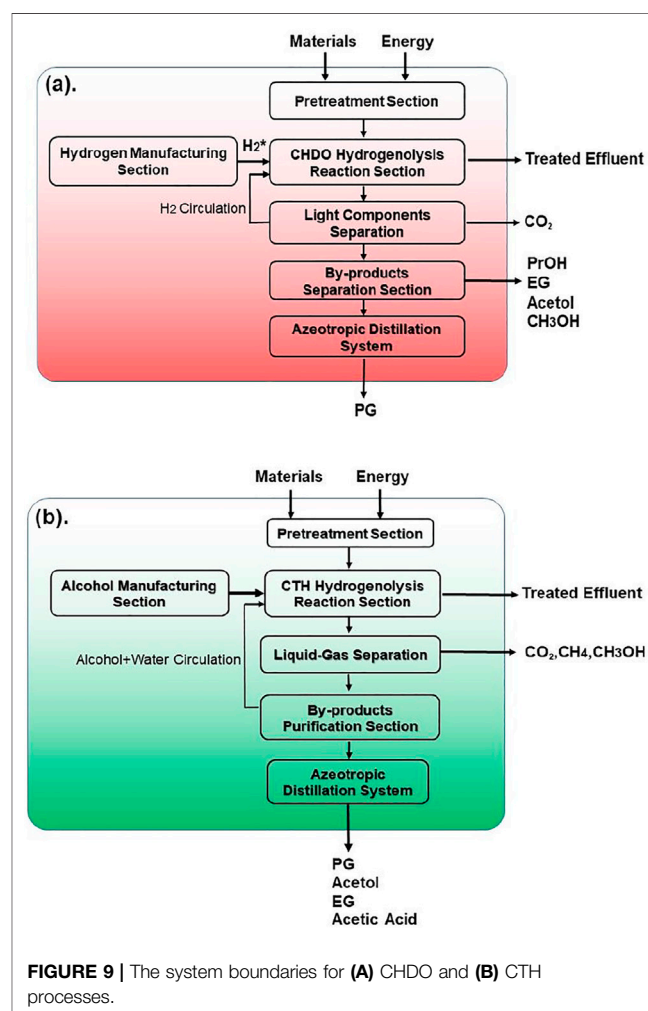


**FIGURE 9 |** The system boundaries for **(A)** CHDO and **(B)** CTH processes.

up to 40wt%, the energy duty for R201, T201, and T202 has been lowered by almost 30, 23, and 54%. This is because higher glycerol concentration actually lowers the energy input for heating up the feedstock, as well as the separating cost of water from reaction mixture. This is one of the key findings in the work.

The effect of reaction temperature on the energy input for pretreatment and reaction sections, as well as separating and purification sections was also studied in the following sections. It is found in **Table 3** that, increasing reaction temperature from 180 to 220°C, energy input for R201 has been enhanced by almost 9-fold. Interestingly, the energy cost for T201-T206 does not vary
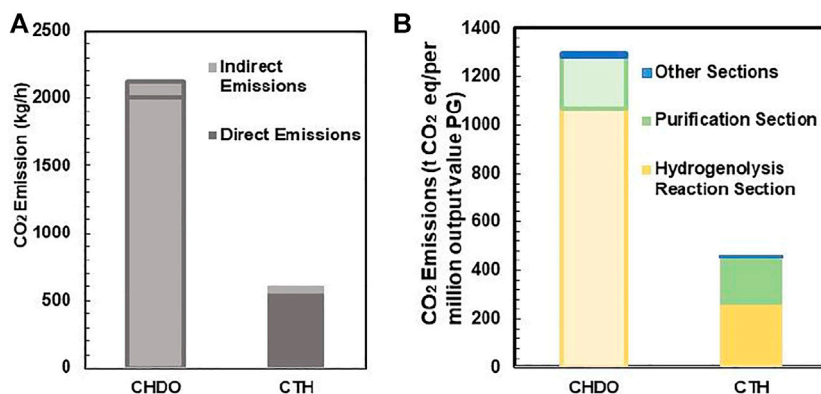
**FIGURE 10 |** The direct and indirect emission of $CO_2$ in CTH and CHDO **(A)**. Equivalent greenhouse gas emissions of CHDO and CTH **(B)**.
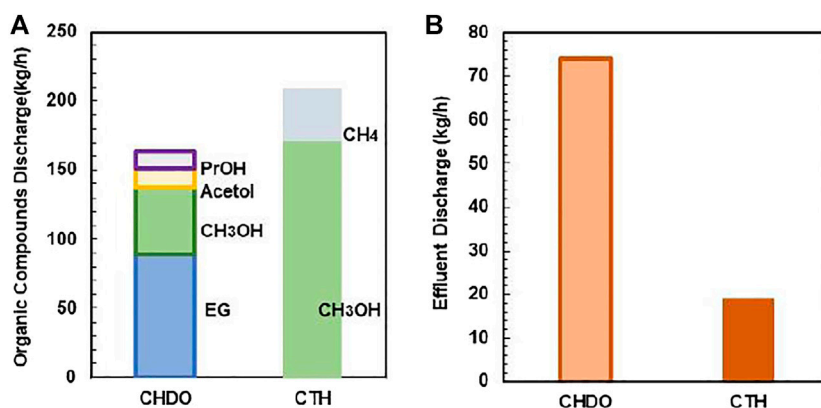


**FIGURE 11 |** The composition of the organic compounds of CHDO and CTH **(A)**. The effluent discharge of CHDO and CTH **(B)**.
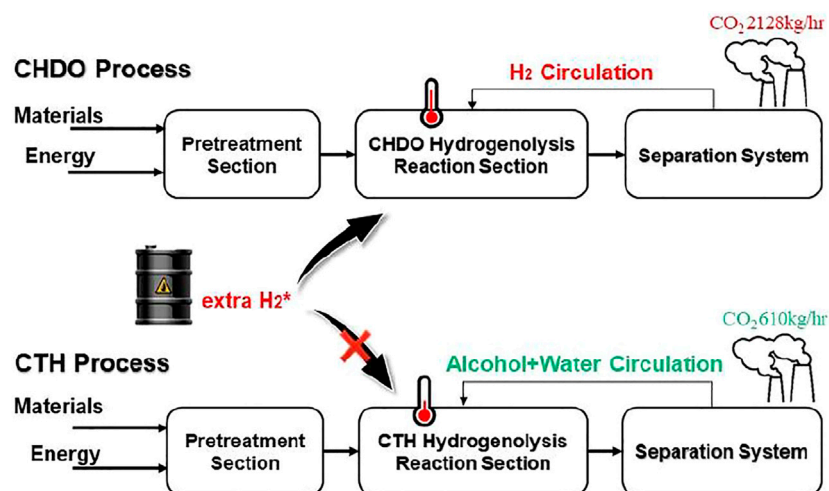


**FIGURE 12 |** The advantages of CTH compared with CHDO.

significantly as expected. However, it is important to mention that changing temperature obviously modifies the reaction rate for both glycerol and EtOH, as well as product distribution. Therefore, the product composition in R201 is significantly different in all three cases in **Table 3** (180°C, 200°C, and 220°C). Detailed information on product composition has already been shown in **Figure 5**. Overall, increasing reaction temperature results in a slight enhancement in energy consumption from 28,116 kW to 31,259 kW. The power consumption for both CTH and CHDO has been shown in **Figure 7**.

## Energy Analysis for Both Schemes

We have selected 20wt% glycerol concentration and 200°C as the reference condition for further process analysis. Energy analysis was conducted to reveal the energy consumption for each unit operation in both CHDO and CTH processes. Specifically, **Table 4** presents the energy summary for material pretreatment, hydrogenolysis, and separation sections in both schemes. It is clear that material pretreatment for CTH process displays slightly lower energy consumption compared with conventional unit (entry#1). Most importantly, reaction unit for CTH shows significantly lower energy requirement (430.4 kW), compared with CHDO (2,247.4 kW). This is because operation temperatures and pressures for CTH process are 200°C and 3 MPa, respectively, which are milder than CHDO scheme (230°C, 3.5 MPa).

For separating and purification sections, we have found that energy requirements for CHDO and CTH schemes are again different from each other. In CHDO process, water, MeOH, and PrOH were obtained from the overhead of T101 column, while the mixture from the bottom of this column contained PG, EG, acetol, and small amounts of water (4wt%). Water has been obtained from the bottom of T102 and recycled back to the mixer in the pretreatment and reaction section, with MeOH/PrOH obtained from overhead of T102. Acetol of 92wt% purity can be produced from T103 as one of the co-products from CHDO process. PG and EG are separated in T104 with cycloheptane as azeotropic agent. EG of 99.97wt% purity can be obtained from T104, while PG of 99.92wt% can be produced from T105. Clearly, the heat duty for T101 is the highest compared with other columns in CHDO scheme. The azeotropic unit consisting of T104 and T105 demands a total energy input of 8,044 kW.

Since the product distribution for CTH is different from that of CHDO, the separating and purification scheme for CTH varies significantly. In particular, T201 separates light gases such as $H_2$ (7wt%), $CH_4$ (9wt%), $CO_2$ (79.8wt%), and MeOH (3wt%) from the product mixture. Alcohol and water mixture was produced from the top of T202 and recycled back to the mixer in hydrogenolysis unit.

Acetol and acetic acid were separated from PG and EG in T203, while purified acetol of 99.9wt% as the highly valuable co-product can be obtained from bottom of T204. Acetic acid of 97wt% purity (containing 0.2wt% acetol and ~2.8wt% water as impurities) was produced from the top of T204. Similar to CHDO process, PG and EG were also separated *via* azeotorpic distillation, in T205 and T206 columns. It can be seen that alcohol and water recycle unit

(T202) demands significantly high energy input in CTH scheme, while for CHDO process, separating water/MeOH/PrOH from product mixture needs remarkably high energy input (T201). The overall energy requirement for purification of acetol, PG, and EG is relatively lower in CTH process compared with CHDO scheme. As a result, the energy requirement for purification unit is 49,597 kW and 42,491 kW for CHDO and CTH, respectively. Considering the advantages of milder operation temperatures and pressures in CTH process, the total energy for the proposed process is 17% lower than CHDO scheme.

## Capital Cost and Revenue

Based on the detailed analysis shown above, we further conducted techno-economic analysis for CHDO and the proposed CTH process, with regard to energy consumption and product distribution. The total number of equipment is summarized in **Supplementary Table S4**. It is found that the overall number of equipment is similar in both schemes, except for flash tank and compressor. This is because CTH process does not require $H_2$ compressor at all, while in CHDO scheme, $H_2$ compressor is a critical unit to recycle excess $H_2$ back to the reaction unit.

Detailed capital investment for CHDO and CTH processes is compared in **Figure 8A**. It is found that the investment for tanks and pumps is similar for both processes. However, due to relatively lower operating pressure in CTH process, the cost for reactor and heat exchangers is lower than that of CHDO. Another important point is that CTH process requires relatively higher investment for separation scheme. This is because several reactions are involved in CTH scheme; thus, additional co-products such as acetic acid and acetol are produced. As a result, the cost for column is slightly more expensive. The overall equipment investment for CTH is more cost-effective than CHDO process. The capital cost of CHDO and CTH schemes is summarized in **Table 5**.

It is important to point out that, since CTH process does not involve use of pressurized $H_2$, the maintenance and safety cost will also be much lower compared with CHDO process. This is because that, in CTH scheme, reactor is conducted under much milder temperature and pressure. As a result, $H_2$ compressor is not needed, with reduced operation cost.

In addition, CTH process produces other co-products including acetol, acetic acid, and EG; therefore, three additional storage tanks are needed. However, the overall cost for the three tanks is obviously lower than $H_2$ tank and compressor.

Detailed cost assignment for different unit operations in CTH process is presented in **Figure 8B**. The key finding in this part is that separation is the main cost contributor in this scheme, where investment for both heat exchangers and columns accounts for as high as 81.6% in CTH process.

According to our detailed simulation on CHDO and CTH processes, the sale revenue for both processes is listed in **Table 6**. We further compared the revenue for various different products including EG, acetic acid, PG, and acetol. Due to the relatively lower product flow rates in CTH scheme, the sales revenue is slightly lower than that of CHDO. However, the lost revenue is trade off by the remarkable price for acetol product. Therefore, the overall revenue is approximately 3-fold higher in CTH scheme.

## Environmental Assessment

The novelty of transfer technologies has been demonstrated in numerous previous work (Sawadjoon et al., 2013). However, quantitative assessment for environmental impact of conventional and the proposed new process has not been investigated comprehensively in current literature. Therefore, in this section, detailed analysis for CHDO and CTH will be conducted and the results will be discussed systematically.

### Boundaries

The boundaries for environmental analysis for both processes are presented in **Figure 9**. For CHDO process (**Figure 9A**), the inlet materials include glycerol and $H_2$. Actually, $H_2$ is industrially derived from fossil fuels using coal or natural gas as the starting material. Therefore, the environmental impact from fossil-$H_2$ generation is also included in this assessment. The leaving materials are mainly consisting of the oxygenate products and waste gases, such as PG, PrOH, EG, acetol, MeOH, and $CO_2$. Differently, the entering materials for CTH process (**Figure 9B**) are mainly glycerol and EtOH, the latter of which can be also derived from bio-substrates. It is important to mention that CTH scheme does not require input of fossil-$H_2$. Due to the complexity of reaction network in CTH process, the by-products are yet different from CHDO. For example, $CH_4$ and acetic acid are main by-products (co-products). The leaving materials in CTH scheme also include PG, acetol, and EG, similar to CHDO process (Garcia-Herrero et al., 2016; Sternberg et al., 2017).

### $CO_2$ Emission per PG Production

Based on process simulation, it is clear that productivity of PG in CTH process is relatively lower compared with CHDO process, due to the co-production of highly valuable acetol. To quantify the $CO_2$ emission, it is important to normalize based on PG production for comparative studies of CHDO and CTH processes.

Emission of $CO_2$ and effluent discharge will be assessed in this section for both processes (Sternberg et al., 2017). The results are presented in **Figure 10**. It can be seen from **Figure 10A** that the sum of indirect and direct $CO_2$ emission for CHDO is almost 5-fold higher than CTH process. Direct $CO_2$ emission is defined as formation of this product from hydrogenation unit and post-treatment of CO as by-product. Therefore, it is not surprising that the direct $CO_2$ emission from CHDO is much higher than that of CTH. Indirect $CO_2$ emission include the $CO_2$ output from process utilities. It is clear that both CHDO and CTH only discharge small amounts of indirect $CO_2$.

Effluent discharge is also compared in this work. Again, the discharge is approximately 73 kg/h for CHDO, which is almost 5-fold higher than CTH scheme. This is because that, in CHDO process, water is the product rather than reactants. Therefore, significant amounts of wastewater are generated under this condition. In CTH process, water is one of the important reactants for $H_2$ generation; as a result, the utilization efficiency is very high. Thus, wastewater discharge is minimized under this circumstance.

The discharge for other organic compounds has also been compared (**Figure 11**). Due to the formation of various other co-products such as $CH_4$, acetic acid, and MeOH, the discharge of organic products is higher in CTH process. This is because we have not considered the purification part for the two chemicals, which can be further improved in future work.

The $CO_2$ emission per million value was eventually compared for CHDO and CTH. It is very critical to mention that acetol is not the hydrogenation product, although the value of which contributes significantly to the final sales revenue. $CO_2$ emission per million value should be evaluated only for hydrogenation product (Xiang et al., 2014; Zhou et al., 2019). In this work, PG is actually the target product for both CHDO and CTH processes. The data presented in **Figure 10** only reflect the $CO_2$ footprint for PG formation. According to the analysis, $CO_2$ output is dramatically higher in CHDO scheme, while that in CTH scheme has been reduced by 71%. Further detailed analysis revealed that, actually contribution of $CO_2$ output from purification and pretreatment section is similar for CHDO and CTH. However, CHDO will release significant amounts of $CO_2$ owing to the harsh operating temperature and $H_2$ pressure. According to the environmental impact analysis, it is clear that our proposed transfer hydrogenolysis technology imposes less carbon footprints in comparison with CHDO process, thus displaying great potentials for large scale implementation in bio-refineries.

## CONCLUSION

In this work, we have conducted detailed analysis for both conventional hydrogenolysis (CHDO) and catalytic transfer hydrogenolysis (CTH) of glycerol processes. Process scheme for both processes has been discussed with respect to energy consumption, productivity, and product distribution. The key finding in this part is that total energy input for CTH of glycerol is approximately 83% of CHDO process. Detailed economic analysis has demonstrated a total reduction of 7% for total investment in CTH scheme, owing to simplification of $H_2$ handling equipment. Furthermore, influence of two critical parameters, glycerol concentration and reactor temperature on energy consumption, recycling water, and productivity for each key product, has been further discussed in detail. As one of the key findings, catalytic transfer hydrogenolysis process demand less energy input compared with conventional processes. More importantly, economic analysis confirmed the advantage of transfer hydrogenolysis due to the reduction of $H_2$ recycling and compression units. Owing to the elimination of natural gas-derived $H_2$ source, the overall $CO_2$ emission in transfer hydrogenolysis has been reduced by more than 71%. Further analysis confirms that a remarkable improvement for CTH over CHDO with a total of 64% reduction in $CO_2$ emission (per $ per production of propylene glycol) has been achieved.

This work has clearly demonstrated the advantages of transfer hydrogenolysis of glycerol to propylene glycol over PtFe-based catalysts. This work will be useful for future process development and implementation of transfer hydrogenolysis technologies in next-generation bio-refineries. The advantages of CTH compared with CHDO are shown in **Figure 12**.

## SUPPORTING INFORMATION

Additional information on process schemes, equipment design, economic analysis, and heat transfer optimization are available in supporting information.

## DATA AVAILABILITY STATEMENT

The original contributions presented in the study are included in the article/**Supplementary Material**. Further inquiries can be directed to the corresponding authors.

## AUTHOR CONTRIBUTIONS

PS, WZ, and XY drafted the paper. JZ, NX, ZZ, ML, and DZ collected information. GZ, ZL, CY, and XJ provided comments and funding.

## FUNDING

## SUPPLEMENTARY MATERIAL

The Supplementary Material for this article can be found online at: https://www.frontiersin.org/articles/10.3389/fchem.2021.778579/full#supplementary-material

## REFERENCES

A, A. A., Mondal, S., Pudi, S. M., Pandhare, N. N., and Biswas, P. (2017). Liquid Phase Hydrogenolysis of Glycerol over Highly Active 50%Cu–Zn(8:2)/MgO Catalyst: Reaction Parameter Optimization by Using Response Surface Methodology. *Energy & Fuels* 31 (8), 8521–8533. doi:10.1021/acs.energyfuels.7b00766

Arpia, A. A., Chen, W.-H., Lam, S. S., Rousset, P., and de Luna, M. D. G. (2021). Sustainable Biofuel and Bioenergy Production from Biomass Waste Residues Using Microwave-Assisted Heating: A Comprehensive Review. *Chem. Eng. J.* 1, 403. doi:10.1016/j.cej.2020.126233

Beneroso, D., Monti, T., Kostas, E. T., and Robinson, J. (2017). Microwave Pyrolysis of Biomass for Bio-Oil Production: Scalable Processing Concepts. *Chem. Eng. J.* 316, 481–498. doi:10.1016/j.cej.2017.01.130

Cai, F., Pan, D., Ibrahim, J. J., Zhang, J., and Xiao, G. (2018). Hydrogenolysis of Glycerol over Supported Bimetallic Ni/Cu Catalysts with and without External Hydrogen Addition in a Fixed-Bed Flow Reactor. *Appl. Catal. A: Gen.* 564, 172–182. doi:10.1016/j.apcata.2018.07.029

Chen, Y., Sun, Y., Yang, Z., Lu, X., and Ji, X. (2020). CO2 Separation Using a Hybrid Choline-2-Pyrrolidine-Carboxylic Acid/polyethylene Glycol/water Absorbent. *Appl. Energ.* 1, 257. doi:10.1016/j.apenergy.2019.113962

Cormos, C.-C. (2021). *Techno-economic Assessment of Calcium and Magnesium-Based Sorbents for post-combustion CO2 Capture Applied in Fossil-Fueled Power Plants*. Cluj-Napoca: Fuel, 298. doi:10.1016/j.fuel.2021.120794

D'Angelo, S. C., Dall'Ara, A., Mondelli, C., Pérez-Ramírez, J., and Papadokonstantakis, S. (2018). Techno-Economic Analysis of a Glycerol Biorefinery. *ACS Sust. Chem. Eng.* 6 (12), 16563–16572. doi:10.1021/acssuschemeng.8b03770

Dohnal, V., Baránková, E., and Blahut, A. (2014). Separation of Methyl Acetate+methanol Azeotropic Mixture Using Ionic Liquid Entrainers. *Chem. Eng. J.* 237, 199–208. doi:10.1016/j.cej.2013.10.011

Falcone, D. D., Hack, J. H., Klyushin, A. Y., Knop-Gericke, A., Schlögl, R., and Davis, R. J. (2015). Evidence for the Bifunctional Nature of Pt-Re Catalysts for Selective Glycerol Hydrogenolysis. *ACS Catal.* 5 (10), 5679–5695. doi:10.1021/acscatal.5b01371

Feng, Y.-S., Liu, C., Kang, Y.-M., Zhou, X.-M., Liu, L.-L., Deng, J., et al. (2015). Selective Hydrogenolysis of Glycerol to 1,2-propanediol Catalyzed by Supported Bimetallic PdCu-Kf/γ-Al2O3. *Chem. Eng. J.* 281, 96–101. doi:10.1016/j.cej.2015.06.087

Feng, Y., Yin, H., Wang, A., Shen, L., Yu, L., and Jiang, T. (2011). Gas Phase Hydrogenolysis of Glycerol Catalyzed by Cu/ZnO/MOx (MOx=Al2O3, TiO2, and ZrO2) Catalysts. *Chem. Eng. J.* 168 (1), 403–412. doi:10.1016/j.cej.2011.01.049

Freitas, I. C., Manfro, R. L., and Souza, M. M. V. M. (2018). Hydrogenolysis of Glycerol to Propylene Glycol in Continuous System without Hydrogen Addition over Cu-Ni Catalysts. *Appl. Catal. B: Environ.* 220, 31–41. doi:10.1016/j.apcatb.2017.08.030

Garcia-Herrero, I., Cuéllar-Franca, R. M., Enríquez-Gutiérrez, V. M., Alvarez-Guerra, M., Irabien, A., and Azapagic, A. (2016). Environmental Assessment of Dimethyl Carbonate Production: Comparison of a Novel Electrosynthesis Route Utilizing CO2 with a Commercial Oxidative Carbonylation Process. *ACS Sust. Chem. Eng.* 4 (4), 2088–2097. doi:10.1021/acssuschemeng.5b01515

Gonzalez-Garay, A., Gonzalez-Miquel, M., and Guillen-Gosalbez, G. (2017). High-Value Propylene Glycol from Low-Value Biodiesel Glycerol: A Techno-Economic and Environmental Assessment under Uncertainty. *ACS Sust. Chem. Eng.* 5 (7), 5723–5732. doi:10.1021/acssuschemeng.7b00286

Guo, X., Li, Y., Shi, R., Liu, Q., Zhan, E., and Shen, W. (2009). Co/MgO Catalysts for Hydrogenolysis of Glycerol to 1, 2-propanediol. *Appl. Catal. A: Gen.* 371 (1-2), 108–113. doi:10.1016/j.apcata.2009.09.037

Haldar, P., and Mahajani, V. V. (2004). Catalytic Transfer Hydrogenation: O-nitro Anisole to O-Anisidine, Some Process Development Aspects. *Chem. Eng. J.* 104 (1-3), 27–33. doi:10.1016/j.cej.2004.08.002

Hernández, A., Cartes, M., and Mejía, A. (2018). Measurement and Modeling of Isobaric Vapor – Liquid Equilibrium and Isothermal Interfacial Tensions of Ethanol + Hexane + 2, 5 – Dimethylfuran Mixture. *Fuel* 229, 105–115. doi:10.1016/j.fuel.2018.04.079

Hu, J., Zhao, M., Jiang, B., Wu, S., and Lu, P. (2020). Catalytic Transfer Hydrogenolysis of Native Lignin to Monomeric Phenols over a Ni-Pd Bimetallic Catalyst. *Energy Fuels* 34 (8), 9754–9762. doi:10.1021/acs.energyfuels.0c01962

Humbird, D., Trendewicz, A., Braun, R., and Dutta, A. (2017). One-Dimensional Biomass Fast Pyrolysis Model with Reaction Kinetics Integrated in an Aspen Plus Biorefinery Process Model. *ACS Sust. Chem. Eng.* 5 (3), 2463–2470. doi:10.1021/acssuschemeng.6b02809

Jin, X., Fang, T., Wang, J., Liu, M., Pan, S., Subramaniam, B., et al. (2019). Nanostructured Metal Catalysts for Selective Hydrogenation and Oxidation of Cellulosic Biomass to Chemicals. *Chem. Rec.* 19 (9), 1952–1994. doi:10.1002/tcr.201800144

Jin, X., Yin, B., Xia, Q., Fang, T., Shen, J., Kuang, L., et al. (2019). Catalytic Transfer Hydrogenation of Biomass-Derived Substrates to Value-Added Chemicals on Dual-Function Catalysts: Opportunities and Challenges. *ChemSusChem* 12 (1), 71–92. doi:10.1002/cssc.201801620

Kant, A., He, Y., Jawad, A., Li, X., Rezaei, F., Smith, J. D., et al. (2017). Hydrogenolysis of Glycerol over Ni, Cu, Zn, and Zr Supported on H-Beta. *Chem. Eng. J.* 317, 1–8. doi:10.1016/j.cej.2017.02.064

Li, H., Xia, S., Luo, H., and Ma, P. (2016). Experimental and Computational Study on the Compatibility of Biodiesel/diesel/methanol Blended Fuel. *Fuel* 173, 52–59. doi:10.1016/j.fuel.2016.01.036

Liu, H., Cai, C., Jia, M., Yan, Y. a., and Xi, X. (2018). Bubble Growth Characteristics in Bi-component Liquid: Influence of Component Concentration and Liquid Temperature. *Chem. Eng. Sci.* 192, 1–15. doi:10.1016/j.ces.2018.07.018

Ma, C., Shukla, S. K., Samikannu, R., Mikkola, J.-P., and Ji, X. (2019). CO2 Separation by a Series of Aqueous Morpholinium-Based Ionic Liquids with

Acetate Anions. *ACS Sust. Chem. Eng.* 8 (1), 415–426. doi:10.1021/acssuschemeng.9b05686

Ma, C., Xie, Y., Ji, X., Liu, C., and Lu, X. (2018). Modeling, Simulation and Evaluation of Biogas Upgrading Using Aqueous Choline Chloride/urea. *Appl. Energ.* 229, 1269–1283. doi:10.1016/j.apenergy.2017.03.059

Marchese, M., Chesta, S., Santarelli, M., and Lanzini, A. (2021). *Techno-economic Feasibility of a Biomass-To-X Plant: Fischer-Tropsch Wax Synthesis from Digestate Gasification*. Turin: Energy, 228. doi:10.1016/j.energy.2021.120581

Mauriello, F., Ariga, H., Musolino, M. G., Pietropaolo, R., Takakusagi, S., and Asakura, K. (2015). Exploring the Catalytic Properties of Supported Palladium Catalysts in the Transfer Hydrogenolysis of Glycerol. *Appl. Catal. B: Environ.* 166-167, 121–131. doi:10.1016/j.apcatb.2014.11.014

Mirzaei, S., Shamiri, A., and Aroua, M. K. (2016). Simulation of Aqueous Blend of Monoethanolamine and Glycerol for Carbon Dioxide Capture from Flue Gas. *Energy Fuels* 30 (11), 9540–9553. doi:10.1021/acs.energyfuels.6b01230

Nie, R., Tao, Y., Nie, Y., Lu, T., Wang, J., Zhang, Y., et al. (2021). Recent Advances in Catalytic Transfer Hydrogenation with Formic Acid over Heterogeneous Transition Metal Catalysts. *ACS Catal.* 11 (3), 1071–1095. doi:10.1021/acscatal.0c04939

Park, Y.-K., Ha, J.-M., Oh, S., and Lee, J. (2021). Bio-oil Upgrading through Hydrogen Transfer Reactions in Supercritical Solvents. *Chem. Eng. J.* 1, 404. doi:10.1016/j.cej.2020.126527

Pla-Franco, J., Lladosa, E., Loras, S., and Montón, J. B. (2019). Azeotropic Distillation for 1-propanol Dehydration with Diisopropyl Ether as Entrainer: Equilibrium Data and Process Simulation. *Sep. Purif. Tech.* 212, 692–698. doi:10.1016/j.seppur.2018.11.082

Poozesh, S., Rayer, A. V., and Henni, A. (2015). Molar Excess Enthalpy (HmE) for Systems of Aqueous Piperazine Derivatives. *The J. Chem. Thermodynamics* 90, 242–250. doi:10.1016/j.jct.2015.06.006

Priya, S. S., Bhanuchander, P., Kumar, V. P., Bhargava, S. K., and Chary, K. V. R. (2016). Activity and Selectivity of Platinum-Copper Bimetallic Catalysts Supported on Mordenite for Glycerol Hydrogenolysis to 1,3-Propanediol. *Ind. Eng. Chem. Res.* 55 (16), 4461–4472. doi:10.1021/acs.iecr.6b00161

Qin, Y., Zhang, H., Liu, S., and Yang, M. (2019). Measurements of Isothermal Vapor-Liquid Equilibrium for 2, 3, 3, 3-Tetrafluoroprop-1-Ene + 1,1,1,2-tetrafluoroethane + Propane System at Temperatures from 283.15 to 323.15 K. *J. Chem. Thermodynamics* 131, 111–116. doi:10.1016/j.jct.2018.10.028

Rocha, E. G. d. A., Follegatti-Romero, L. A., Duvoisin, S., and Aznar, M. (2014). Liquid-liquid Equilibria for Ternary Systems Containing Ethylic palm Oil Biodiesel+ethanol+glycerol/water: Experimental Data at 298.15 and 323.15K and Thermodynamic Modeling. *Fuel* 128, 356–365. doi:10.1016/j.fuel.2014.01.074

Saavedra del Oso, M., Mauricio-Iglesias, M., and Hospido, A. (2020). Evaluation and Optimization of the Environmental Performance of PHA Downstream Processing. *Chem. Eng. J.* 1, 1. doi:10.1016/j.cej.2020.127687

Sawadjoon, S., Lundstedt, A., and Samec, J. S. M. (2013). Pd-Catalyzed Transfer Hydrogenolysis of Primary, Secondary, and Tertiary Benzylic Alcohols by Formic Acid: A Mechanistic Study. *ACS Catal.* 3 (4), 635–642. doi:10.1021/cs300785r

Shafaghat, H., Lee, I.-G., Jae, J., Jung, S.-C., and Park, Y.-K. (2019). Pd/C Catalyzed Transfer Hydrogenation of Pyrolysis Oil Using 2-propanol as Hydrogen Source. *Chem. Eng. J.* 377, 1. doi:10.1016/j.cej.2018.09.147

Song, Q., David Wang, W., Lu, K., Li, F., Wang, B., Sun, L., et al. (2021). Three-dimensional Hydrophobic Porous Organic Polymers Confined Pd Nanoclusters for Phase-Transfer Catalytic Hydrogenation of Nitroarenes in Water. *Chem. Eng. J.* 1, 415. doi:10.1016/j.cej.2021.128856

Sternberg, A., Jens, C. M., and Bardow, A. (2017). Life Cycle Assessment of CO2-based C1-Chemicals. *Green. Chem.* 19, 2244–2259. doi:10.1039/c6gc02852g

Sun, Q., Wang, S., and Liu, H. (2017). Selective Hydrogenolysis of Glycerol to Propylene Glycol on Supported Pd Catalysts: Promoting Effects of ZnO and Mechanistic Assessment of Active PdZn Alloy Surfaces. *ACS Catal.* 7 (7), 4265–4275. doi:10.1021/acscatal.7b00995

Tike, M. A., and Mahajani, V. V. (2006). Studies in Catalytic Transfer Hydrogenation of Soybean Oil Using Ammonium Formate as Donor over 5% Pd/C Catalyst. *Chem. Eng. J.* 123 (1-2), 31–41. doi:10.1016/j.cej.2006.07.014

Vasiliadou, E. S., and Lemonidou, A. A. (2013). Kinetic Study of Liquid-phase Glycerol Hydrogenolysis over Cu/SiO2 Catalyst. *Chem. Eng. J.* 231, 103–112. doi:10.1016/j.cej.2013.06.096

Von Held Soares, A., Atia, H., Armbruster, U., Passos, F. B., and Martin, A. (2017). Platinum, Palladium and Nickel Supported on Fe 3 O 4 as Catalysts for Glycerol Aqueous-phase Hydrogenation and Reforming. *Appl. Catal. A: Gen.* 548, 179–190. doi:10.1016/j.apcata.2017.07.023

Wang, C., Jiang, H., Chen, C., Chen, R., and Xing, W. (2015). Solvent Effect on Hydrogenolysis of Glycerol to 1,2-propanediol over Cu-ZnO Catalyst. *Chem. Eng. J.* 264, 344–350. doi:10.1016/j.cej.2014.11.113

Wang, S., Yin, K., Zhang, Y., and Liu, H. (2013). Glycerol Hydrogenolysis to Propylene Glycol and Ethylene Glycol on Zirconia Supported Noble Metal Catalysts. *ACS Catal.* 3 (9), 2112–2121. doi:10.1021/cs400486z

Wang, Y., Zhou, J., and Guo, X. (2015). Catalytic Hydrogenolysis of Glycerol to Propanediols: a Review. *RSC Adv.* 5 (91), 74611–74628. doi:10.1039/c5ra11957j

Wicker, R. J., Kumar, G., Khan, E., and Bhatnagar, A. (2021). Emergent green Technologies for Cost-Effective Valorization of Microalgal Biomass to Renewable Fuel Products under a Biorefinery Scheme. *Chem. Eng. J.* 1, 415. doi:10.1016/j.cej.2021.128932

Xia, Q., Zhang, G., Wang, J., Zhang, W., Liu, M., Li, Y., et al. (2020). Synergistic Bimetallic Pd-Pt/TiO2 Catalysts for Hydrogenolysis of Xylitol with In Situ-Formed H2. *Ind. Eng. Chem. Res.* 59 (31), 13879–13891. doi:10.1021/acs.iecr.0c01564

Xiang, D., Qian, Y., Man, Y., and Yang, S. (2014). Techno-economic Analysis of the Coal-To-Olefins Process in Comparison with the Oil-To-Olefins Process. *Appl. Energ.* 113, 639–647. doi:10.1016/j.apenergy.2013.08.013

Xie, Y., Dong, H., Zhang, S., Lu, X., and Ji, X. (2016). Solubilities of CO2, CH4, H2, CO and N2 in Choline Chloride/urea. *Green. Energ. Environ.* 1 (3), 195–200. doi:10.1016/j.gee.2016.09.001

Yin, B., Jin, X., Zhang, G., Yan, H., Zhang, W., Liu, X., et al. (2020). Catalytic Transfer Hydrogenolysis of Bio-Polyols to Renewable Chemicals over Bimetallic PtPd/C Catalysts: Size-dependent Activity and Selectivity. *ACS Sust. Chem. Eng.* 8 (13), 5305–5316. doi:10.1021/acssuschemeng.0c00524

Zaimes, G. G., Soratana, K., Harden, C. L., Landis, A. E., and Khanna, V. (2015). Biofuels via Fast Pyrolysis of Perennial Grasses: A Life Cycle Evaluation of Energy Consumption and Greenhouse Gas Emissions. *Environ. Sci. Technol.* 49 (16), 10007–10018. doi:10.1021/acs.est.5b00129

Zhang, G., Jin, X., Wang, J., Liu, M., Zhang, W., Gao, Y., et al. (2020). Fe3+-Mediated Pt/Y Zeolite Catalysts Display Enhanced Metal-Bronsted Acid Interaction and Synergistic Cascade Hydrogenolysis Reactions. *Ind. Eng. Chem. Res.* 59 (39), 17387–17398. doi:10.1021/acs.iecr.0c01971

Zhang, G., Jin, X., Zhang, Q., Cheng, Y., Chen, X., Liu, Y., et al. (2020). PtRu/Zn3Ce1Ox Catalysts with Lewis Acid-Base Pairs Show Synergistic Performances for the Conversion of Glycerol in the Absence of Externally Added H2. *Catal. Sci. Technol.* 10 (13), 4386–4395. doi:10.1039/c9cy02465d

Zhao, Z., Jiang, J., Zheng, M., and Wang, F. (2021). Advancing Development of Biochemicals through the Comprehensive Evaluation of Bio-Ethylene Glycol. *Chem. Eng. J.* 1, 411. doi:10.1016/j.cej.2021.128516

Zhou, X., Zhao, H., Feng, X., Chen, X., and Yang, C. (2019). Hydrogenation and TMP Coupling Process: Novel Process Design, Techno-Economic Analysis, Environmental Assessment and Thermo-Economic Optimization. *Ind. Eng. Chem. Res.* 58 (24), 10482–10494. doi:10.1021/acs.iecr.9b01681